Growth of fatigue cracks subjected to non-proportional Mode I and II

Peter Dahlin

Doctoral Thesis no. 61
Solid Mechanics
KTH Engineering Sciences
SE-100 44 Stockholm, Sweden

TRITA HFL-0398
ISSN 1104-6813
ISRN KTH/HFL/R--05/14--SE
ISBN 91-7178-241-9

Akademisk avhandling som med tillstånd av Kungliga Tekniska Högskolan i Stockholm framlägges till offentlig granskning för avläggande av teknisk doktorsexamen tisdagen den 24 januari kl. 10.15 i sal F3, Kungliga Tekniska Högskolan, Lindstedtsvägen 28, Stockholm.

PREFACE

This work was carried out at the Department of Solid Mechanics, Royal Institute of Technology, Stockholm, Sweden. Financial support was provided by the Swedish Research Council (VR). This support is gratefully acknowledged.

I would like to convey my sincere gratitude to:

My supervisor, Assoc. Prof. **Mårten Olsson**, for excellent guidance during the course of the work. For your endless support and patience during these years.

Mr. **Hans Öberg** for all the help with the experiments and measurements, and for designing the loading device used in paper D. Mr. **Bertil Dolk** for manufacturing the specimens and for building the loading device used in paper D.

Mr. **Kaj Pettersson** for making all the traveling back and forth to Uppsala much more pleasant due to conversations about all sorts of things from fracture mechanics to fishing and house redecoration. Thank you also for the valuable comments on the Introduction of this thesis. Mr. **Alessandro Cadario**, my room mate at the department for almost four years, for assistance, support and valuable discussions. All present and former **colleagues** at the department for creating a stimulating atmosphere, for enjoyable dissertation parties and for all activities we have practiced, floor ball, running (Hookes lag), golf, sailing and kayaking.

My parents, **Nisse** and **Marika** and my sister **Gabriella** for all the support.

Finally, I would like to thank my beloved **Camilla**, for all your love and support.

Uppsala in December 2005

Peter Dahlin

DISSERTATION

This dissertation consists of a summary and the following papers:

[A] P. Dahlin and M. Olsson (2003). The effect of plasticity on incipient mixed-mode fatigue crack growth. Fatigue Fract. Engng Mater. Structs, **26**, 577-588.

[B] P. Dahlin and M. Olsson (2004). Reduction of mode I fatigue crack growth rate due to occasional mode II loading. Int. J. Fatigue, **26**, 1083-1093.

[C] P. Dahlin and M. Olsson. Mode I fatigue crack growth reduction mechanisms after a single mode II load cycle. Report 399, KTH Solid Mechanics, Stockholm, Sweden (2005).

[D] P. Dahlin and M. Olsson. Fatigue crack growth - mode I cycles with periodic mode II loading. Report 400, KTH Solid Mechanics, Stockholm, Sweden (2005).

ABSTRACT

This thesis deals with some aspects of crack growth in the presence of cyclic loading, *i.e.* fatigue. The cyclic load cases studied here are primary of non-proportional mixed mode type. Under non-proportional loading the principal stress directions rotate and, generally, the ratio between the principal stresses vary. A new criterion has been presented for prediction of incipient crack path direction after changes in load from steady Mode I to non-proportional loading. The criterion is based on FE-simulations which are used to compute the actual elasto-plastic stress state in the vicinity of the crack tip. The predictions of the criterion capture several phenomena observed in the literature, which indicates that plasticity effects have to be included in a criterion for crack path predictions under non-proportional loading.

The effects of Mode II overloads on subsequent Mode I crack growth have been studied relatively little in the literature. Also, the results deviates substantially. In the present thesis, this load case has been investigated in detail, both experimentally and analytically. The results show that the Mode I crack growth rate decreases after a single Mode II load, if the *R*-ratio is not as high as to keep the entire Mode I load cycle above the closure level. This is based on the fact, shown in this thesis, that the reduction is caused by crack closure due to tangential displacement of crack-surface irregularities.

A new loading device is presented. With this device, it is possible to apply sequential loading in Mode I and Mode II in an automated way, without having to dismount the specimens. This loading device is used to study the influence of periodic Mode II loading on Mode I crack growth. The main parameters concerning the influence of periodic Mode II loading on Mode I crack growth are; (i) the Mode I *R*-ratio, (ii) the Mode II magnitude and (iii) the Mode II periodicity, *M* (number of Mode I loads for every Mode II load). The mechanisms involved are mainly RICC (Roughness-Induced Crack Closure) and a Mode II mechanism that increases the growth rate temporary at every Mode II load. Hence, the latter becomes more significant for low *M*-values. The higher the Mode I *R*-ratio the smaller is the reduction.

Keywords: Fatigue crack growth, Mode II overloading, Crack closure, Sequential mixed mode loading.

Contents

1. INTRODUCTION

The subject of this thesis is fatigue in metals. In short, fatigue in metals can be summarized as crack initiation and crack growth due to repeated loading. The fatigue subject is huge and this thesis gives a small contribution to a sub-topic within the wider area. What the contribution is will hopefully become obvious in the following.

The load levels required for fatigue are well below the level causing static fracture. Failures can be harmless but also very serious leading to economic losses and in worst case losses of human lives. Examples of the latter kind are failure of vital components in power plants, aeroplanes, ships and other kinds of vehicles. A well known aircraft accident is shown in Fig 1.

Traditional methods to design against fatigue failure are based on infinite fatigue life, which often leads to unnecessary conservatism. More sophisticated methods, in this sense, are usually based on fatigue crack growth, where a crack is allowed to propagate to a certain critical size. This leads to finite fatigue life and an opportunity to optimize the amount of material used for each component. Obvious motivations for this are to reduce weight and material cost. The finite-life approach demands high accuracy of the crack growth rate predictions. Fracture mechanics is known to provide a successful tool for characterizing fatigue crack growth and prediction of failure in components. A large proportion of components and structures in engineering are subjected to complex repeated multi axial loadings and such loadings generally result in a non-proportional stress history. Multi axial fatigue means that more than one loading mode is involved, the loading modes are discussed in Section 2. In multi axial fatigue, the loading history can be either proportional, resulting in alternating stresses or strains having fixed principal directions, or non-proportional where the principal directions and the ratio of the principal stresses vary. A definite criterion for prediction of multi axial fatigue with general applicability is lacking.

Figure 1 Aloha Airlines Boeing 737-297, registration N73711, operating flight AQ243 from Hilo to Honolulu at Kahului Airport on April 28, 1988 after its fuselage was torn away during flight [1].

2. FRACTURE MECHANICS

Fracture occurs in all real materials with various types of material behavior. The simplest material model that realistically mimics the actual behavior of real materials used for design is the isotropic linear elastic model. Fracture mechanics with such material behavior employed is called linear elastic fracture mechanics (LEFM). Using the concept of LEFM a set of loading parameters that describes the crack tip state in a linearly elastic cracked body can be determined. However, there are not many materials that behave elastic at a sharp crack tip, where the stresses are high. The actual stresses at the crack tip in a real material is limited, for instance by the yield stress, σ_Y. A plastic zone will then form at the crack tip. If this plastic zone is sufficiently small it will be embedded within the elastic stress singularity field and LEFM is still applicable. The linear elastic analysis becomes increasingly inaccurate as the inelastic region at the crack tip grows. Assuming linear elastic material behavior, the stress field in a cracked body, expressed in a polar coordinate system with the origin located at the crack tip, can be written as

$$\sigma_{ij} = \frac{A}{\sqrt{r}} f_{ij}(\theta) + \text{H.O.T}, \tag{1}$$

where σ_{ij} is the stress tensor, r and θ are polar coordinates, A is a constant, and f_{ij} is a dimensionless function of θ. The higher order terms, H.O.T, are not that important for

the fracture process. As $r \to 0$, *i.e.* near the crack tip, the stresses varies as $r^{-1/2}$, regardless of the configuration of the cracked body. There are three types of loading which the crack can be exposed to, shown in Fig. 2. Each loading mode gives rise to a $r^{-1/2}$ singularity at the crack tip, but the constant A and the function f_{ij} depend on the loading mode. By replacing the constant A with the stress intensity factor, K, where $K = A\sqrt{2\pi}$, and denote the mode of loading with a subscript, *i.e.* K_I, K_{II} and K_{III}, the stress field ahead of the crack tip can, for small r, be written as

$$\sigma_{ij} = \frac{K_I}{\sqrt{2\pi r}} f_{ij}^{(I)}(\theta) + \frac{K_{II}}{\sqrt{2\pi r}} f_{ij}^{(II)}(\theta) + \frac{K_{III}}{\sqrt{2\pi r}} f_{ij}^{(III)}(\theta) + \text{H.O.T.} \quad (2)$$

Under cyclic loading of cracks, LEFM has proven to be very good for the characterization of the fatigue process in the near-tip region. It should be noted that details of the mechanisms activated inside the fatigue process zone are largely unknown, extremely complicated and not even close to being linearly elastic. The idea of LEFM is that stress intensity factors can still be used as loading measures applied to the fatigue process zone from the outside. This is the case in fatigue and was first experimentally recognized by Paris *et al.* [2]. At very high loading LEFM may not be appropriate for fatigue crack growth analyses. Such high loads are not considered in the present thesis. Hence, this thesis is based on the theory of LEFM, *i.e.* crack tip conditions will be defined by the stress intensity factors.

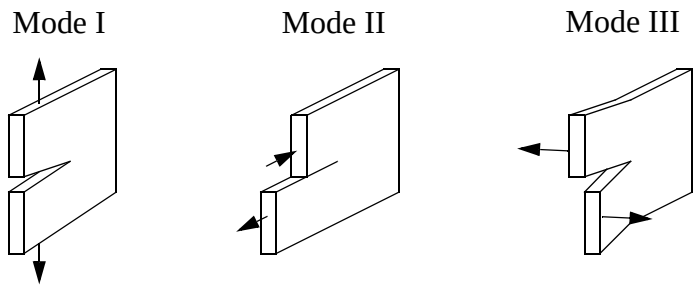

Figure 2 The three loading modes of a crack.

In order to make this theory useful, relations between the remote loads and the stress intensity factors K_I, K_{II} and K_{III} have to be determined, analytically or numerically. The specimen geometry used in the experiments performed in the present thesis requires numerical treatment and the FEM was chosen. In FE-analysis, there are several techniques that can be used to determine stress intensity factors. A stable method is to use domain integrals for a region surrounding the crack tip. The FE-programme used in this thesis, ABAQUS [3], has a built-in routine that utilizes a domain version of the *J*-integral. The value of *J* is related to a combination of the stress intensity factors. The individual stress intensity factors can be found by adding known comparison stress solutions to the numerically found stress field. When plane problems are considered, *i.e.* $K_{III} = 0$, two values of *J* are computed. First, the value of *J* for the numerically found stress field is determined. Then, *J* for the sum of the numerically found stresses and the known comparison field is determined. These two values give K_I and K_{II} for a certain remote load and a certain crack length.

3. MICROSCOPIC STAGES OF FATIGUE

The process of fatigue is characterized by three stages: (i) Crack initiation, where a small crack forms at some point where the stresses are high. The nucleation process for undamaged materials can be described by the intrusion-extrusion mechanism, shown in Fig. 3. Slip bands are formed as a result of dislocation movement within individual grains. Each grain will have a different preferred slip plane depending on the crystal structure. At low stresses, only a few grains have favorable orientations, where the shear stresses are high enough to initiate plastic deformation, and only a few slip bands form. At high stresses, plastic deformation occurs in many grains, and a large number of slip bands form. During repeated cyclic loading, the slip is working back and fourth on the slip bands and eventually a fatigue crack is formed along the persistent slip band. Fatigue crack nucleation often takes place on the surface of a repeatedly loaded body. (ii) Stage I, as long as the crack and the crack tip plastic zone are contained within a few grains, the crack growth occurs predominantly by single shear, in the direction of the primary slip system, see Fig. 4. (iii) Stage II, at this stage the size of the plastic zone at the crack tip contains many grains. On the micro level the crack growth process involves simultaneous or alternating flow along two slip systems. On the macro scale a stage II crack propagates perpendicular to the loading direction, see Fig. 4, if the loading is proportional. This thesis is only concerned with cracks that are well into stage II.

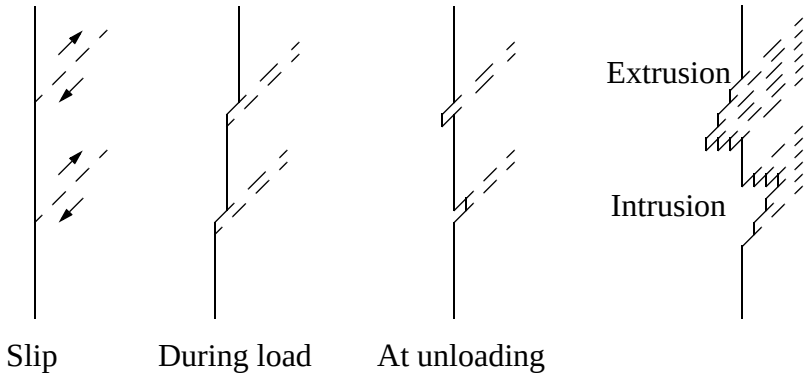

Figure 3 Schematic of the slip band formation in a single grain. The external loading is acting vertically, in tension-compression cycling.

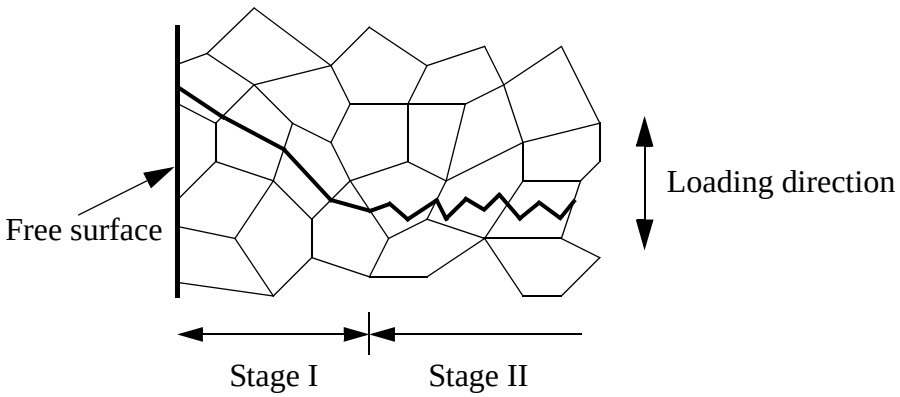

Figure 4 The stage I and stage II crack growth processes in a polycrystalline material.

4. FATIGUE CRACK PROPAGATION AND CRACK CLOSURE

A typical behavior of long Mode I fatigue crack propagation in stage II in ductile metals is illustrated in Fig. 5a. Three regimes of crack growth can be identified, A, B and C. Regime A, is associated with small growth rates, for load ranges below ΔK_{Ith} (a threshold value) no stage II crack growth is observed, above the threshold, da/dN increases rapidly with increased ΔK. Regime C pertains to high load levels, when K_{Imax}

approaches the fracture toughness, K_{IC}, crack growth acceleration is observed. At intermediate ΔK_I-values, regime B, the log-log curve is linear, see Fig. 5a. This region of the curve can be described by a power law function, known as Paris law [2],

$$\frac{da}{dN} = C \cdot \Delta K^m, \tag{1}$$

where C and m are curve fit parameters. This simple expression is however not generally applicable. The fatigue crack growth rate exhibits an R-ratio dependence ($R = K_{min} / K_{max}$), which results in an R-ratio dependence of the parameters C and m and also ΔK_{Ith}, see Fig. 5b. In ductile alloys such as low strength structural materials, the maximum stress intensity factor value corresponding to the fatigue threshold, ΔK_{Ith}, is only a small fraction of the fracture toughness K_{IC}. Table 1 lists the characteristics of the crack propagation in regime A, B and C.

TABLE 1. Characteristics of the three regimes of fatigue crack propagation.

Regime	A	B	C
Microscopic failure mechanisms	Stage I, single shear, faceted or serrated fracture surface	Stage II, duplex shear, striation, planar fracture surface with ripples	Additional cleavage and/or micro void coalescence
Microstructural effects	Large	Small	Large
R-ratio effects	Large	Small	Large
Environmental effects	Large	Large for certain combinations of environment, *R*-ratio and frequency	Small

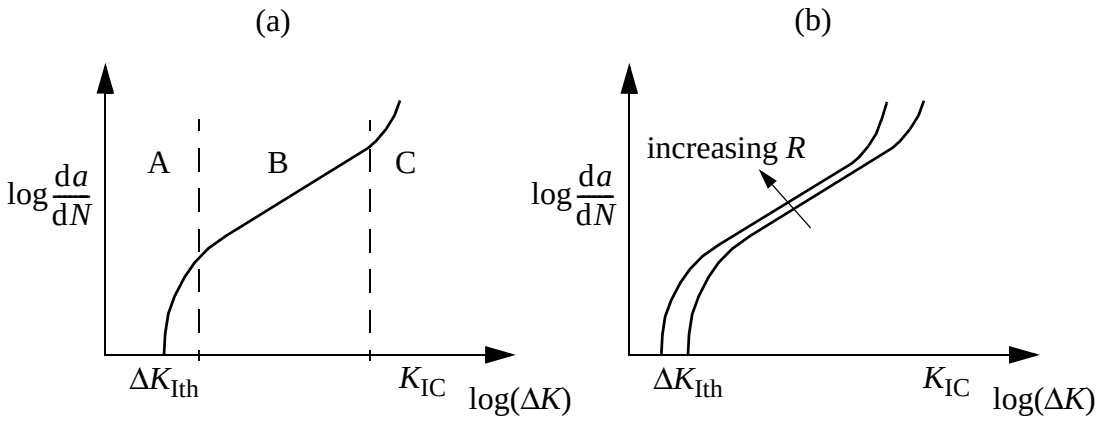

Figure 5 Typical fatigue crack growth behavior in ductile metals (a) showing the three propagation regimes (b) the *R*-ratio effect.

In 1970 Elber [4] introduced the concept of crack closure. He observed that the plastic wake behind the crack tip results in contact between the crack faces before the unloaded state is reached. Thus the crack tip does not experience the full load range, ΔK_{I}. Crack closure decreases the fatigue crack growth rate by reducing the effective stress intensity factor range. The effective stress factor intensity range is defined as:

$$\Delta K_{\mathrm{Ieff}} = \begin{cases} K_{\mathrm{Imax}} - K_{\mathrm{Iclosure}}, & \text{if } K_{\mathrm{Iclosure}} > K_{\mathrm{Imin}} \\ \Delta K_{\mathrm{I}}, & \text{if } K_{\mathrm{Imin}} > K_{\mathrm{Iclosure}} \end{cases} \tag{2}$$

The *R*-ratio dependence should then disappear when ΔK is replaced by ΔK_{Ieff} in Equation (1). By accounting for crack closure, both the fatigue threshold and overload effects can be explained, which will be discussed in Section 4.4. Crack closure can result from several sources [5], the most discussed are plasticity-, roughness- and oxide-induced closure, see Fig. 6.

Plasticity-induced crack closure (PICC), Fig. 6a, can be explained from the history of the crack. When the crack grows, it leaves a wake of plastically stretched material attached to the upper and lower surfaces of the crack, which will make contact before the unloaded state is reached. This reduces the effective load range.

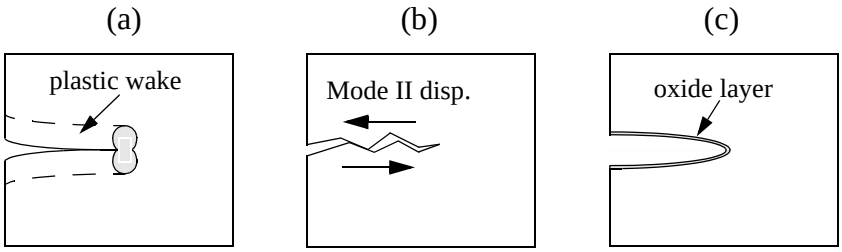

Figure 6 (a) Plasticity-induced closure (b) Roughness-induced closure due to Mode II displacements (c) Oxide-induced closure due an oxide layer.

Roughness-induced crack closure (RICC) is influenced by the microstructure. Although fatigue cracks propagate in pure Mode I conditions on a global scale, crack deflections due to microstructural heterogeneity can lead to mixed mode conditions on the microscopic level. When the crack path deviates from the Mode I symmetry plane, the crack is subjected to Mode II displacements, see Fig. 6b. These displacements cause mismatch between upper and lower crack faces, which in turn results in surface contact before zero load. At low load levels, near the threshold ΔK_{Ith}, where the maximum plastic zone size is typically smaller than a characteristic microstructural dimension such as the grain size, a crystallographic fracture process is promoted. Then the crack only change direction when it encounters a barrier such as a grain boundary. The fatigue crack growth rate in this region is strongly influenced by the grain size, here coarser-grained materials produce rougher fracture surfaces which result in higher closure levels, which in turn increase the threshold value.

Oxide-induced crack closure (OICC), Fig. 6c, is a near-threshold mechanism which is of interest when the thickness of the crack-surface oxide layers is significant in comparison to the crack opening displacement. During the propagation of a fatigue crack, the presence of a moist atmosphere leads to oxidation of the freshly formed fracture surfaces. At low *R*-ratios and low load levels, near the threshold ΔK_{Ith}, the crack face contact is high, as a consequence of local Mode II displacements of fracture surface roughness and PICC. This results in wearing between the crack faces. For low strength steel, this wear mechanism can in laboratory air lead to the build-up of oxide layers which are about 20 times thicker than that formed on a freshly prepared surface which is exposed to the same environment [5]. In comparison, at low *R*-ratios the maximum

crack opening displacement near the threshold for most low-strength steels is in the same order as the built-up oxide layer mentioned above, which naturally leads to an enhanced closure level. At high *R*-ratios significantly less oxidation takes place even near the threshold regime. In Fig. 7, the near-threshold crack propagation in moist laboratory air and in a dehumidified ultra high purity hydrogen environment are shown at $R = 0.05$ and 0.75. The dehumidified ultra high purity hydrogen environment is supposed to minimize the oxidation process. At the low *R*-ratio, the difference in ΔK_{Ith} is significant between the two environments due to the oxide layer that is built up in the moist air test. At the high *R*-ratio, oxide-induced crack closure is almost non-existing in both environments due to the large minimum crack opening displacement (at K_{min}), thus ΔK_{Ith} are about the same. Note, that OICC is a near-threshold mechanism, in general cracks grow faster in a corrosive environment than in vacuum.

A number of experimental techniques for the determination of the closure level in fatigue are available, some of them are given by Donald and Paris [6]. Numerical and analytical methods are also available to estimate the plasticity-induced closure load. The FE-method is a convenient numerical tool [7, 8, 9]. The most common analytical approaches are based on the Dugdale strip-yield model, for example models developed by Budiansky and Hutchinson [10], and Newman [11].

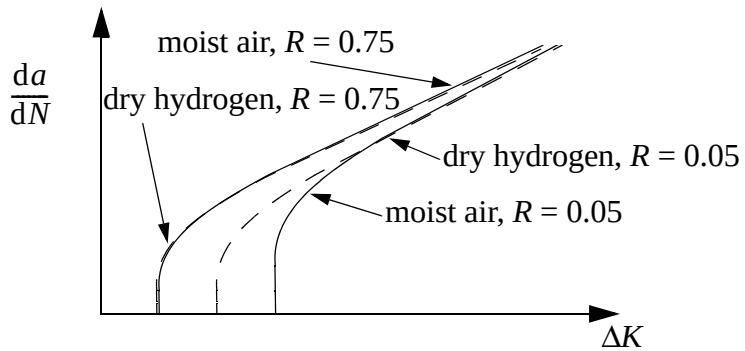

Figure 7 Schematic of the effect of dry and moist environments on near threshold fatigue crack growth, taken from experimental results presented by Suresh [5] in steel (AISI A542 Class 2).

4.1 Crack closure measurements

One of the most common procedures to determine the closure level experimentally is to study load-displacement relations. The crack mouth opening displacement is often used in this relation, see Fig. 8. If there is crack closure, the curve will exhibit a non-linearity, see Fig. 9a. During unloading the load-displacement relation is linear as long as the crack is fully open, when the crack starts to close this linear relation shifts to non-linear. Closure is a continuous process, which means that there is often a significant load interval where the crack is partially closed. The closure load can be defined by deviation in linearity from either the fully closed compliance (at P_{cl1} and below) or the fully open compliance (at P_{cl3} and above), or by extrapolating the fully closed and fully open compliance curves and estimate their intersection (P_{cl2}). There are number of methods suggested to find the closure load from the load-displacement curve [6]. Another procedure to determine the closure level is the so called potential drop technique (PD). The principle of PD is to lead a constant electrical current through the specimen from one side of the crack mouth to the other and measure the electrical potential drop between two points on opposite side of the crack mouth. As the crack length increases so does the electrical resistance, resulting in an increased PD signal, see Fig. 9b.

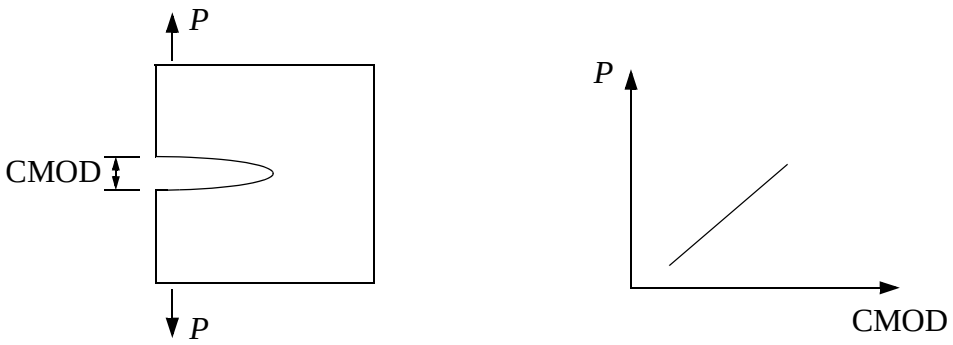

Figure 8 Schematic of the relation between CMOD and applied load, *P*.

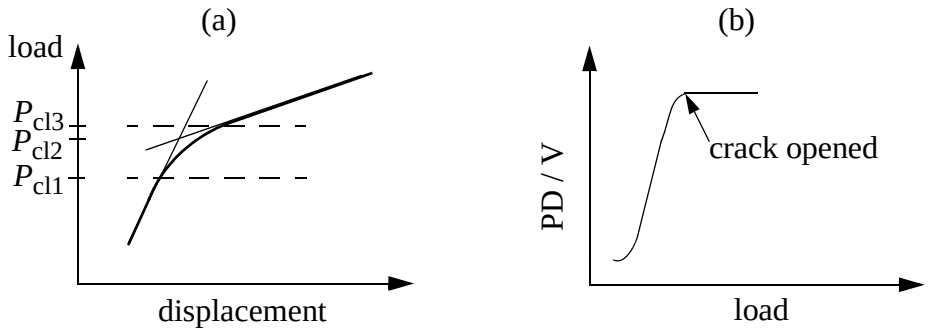

Figure 9 (a) Three definitions of the closure level from the compliance method (b) Crack opening load estimation using potential drop technique.

4.2 Numerical modelling of PICC

The FE-approach is basically to apply a cyclic load to a structure containing a crack and propagate the crack by releasing nodes along the hypothetical crack path. Careful attention must be paid to a series of critical decisions about mesh and model design if the analysis is to be reliable [7]. Usually one node is released per cycle. The material model has to be elasto-plastic, appropriately with kinematic type hardening, in order to capture the residual strains which is the origin of PICC. The element size in the near crack tip region must be very small in order to reproduce the cyclic plastic zone accurately. Advantages of using finite elements are the possibility of 3D-modelling and also the possibility to use advanced material models. The drawback is that it is very time consuming since a cycle-by-cycle simulation is necessary.

4.3 Analytical modelling of PICC

The main assumptions of the analytical model developed by Budiansky and Hutchinson [10] are the following. Steady-state crack growth under plane stress, small scale yielding conditions and constant K_{max}. The crack opening displacement is estimated from a Dugdale analysis, with a residual stretch, δ_R, attached to the crack faces. As the crack grows, it leaves a wake of plastically stretched material attached to the upper and lower surfaces of the crack, which will make contact before the unloaded state is reached. In the near crack tip region, the residual displacements are determined by the reversed plastic flow zone. Ahead of the crack tip, beyond the reversed plastic zone, the

plastic stretch created at $K = K_{max}$ is unchanged during unloading. The Dugdale solution results in a plastic zone size (r_p) and crack tip opening displacement (δ_0) as:

$$r_p = \frac{\pi}{8}\left(\frac{K}{\sigma_Y}\right)^2 \quad \text{and} \quad \delta_0 = \frac{K^2}{\sigma_Y E}. \tag{3}$$

A Cartesian-coordinate system is introduced with the origin located at the crack tip, wherein the crack lies along the negative *x*-axis. A schematic of the problem formulation [10] is shown in Fig. 10. The plastic stretch variation over the distance (0, r_p) is then given by:

$$\frac{\delta}{\delta_0} = g\left(\frac{x}{r_p}\right) \quad \text{where} \quad g(\xi) = \sqrt{1-\xi} - \frac{\xi}{2}\log\left|\frac{1+\sqrt{1-\xi}}{1-\sqrt{1-\xi}}\right| \tag{4)-(5}$$

and $\xi = x/r_p$. Compressive yielding occurs over the distance, $r_c = r_p/4$, during unloading from K_{max}. This results in the following expression for the residual plastic stretch at $K = K_{min} = 0$ over the interval (0, $r_p/4$):

$$\frac{\delta}{\delta_0} = g\left(\frac{x}{r_p}\right) - \frac{1}{2}g\left(\frac{4x}{r_p}\right) \tag{6}$$

where δ_0 is the crack tip opening displacement at K_{max}. The crack-tip stretch ($\delta(x = 0)$ in Eq. 6) at $K_{min} = 0$ is half the value it had at K_{max}.

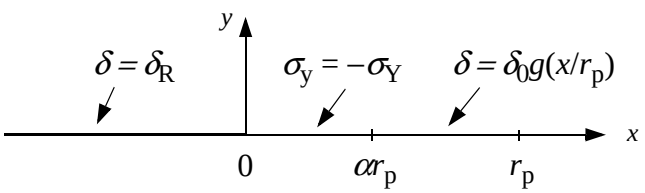

Figure 10 Problem formulation, conditions after unloading, $K = K_{min} = 0$, are shown.

Budiansky and Hutchinson [10] assume that for steady-state crack growth a plastic stretch of magnitude $\delta_R/2$ is attached to the upper and lower crack faces. Using Mushkelishvilis complex potentials formulation with the assumptions mentioned above, it can be shown that this approximation leads to the following expression for the residual plastic stretch [10] in the interval (r_c, r_p):

$$\frac{\delta_R}{\delta_0} = \frac{\pi^2\alpha}{4} + \int_\alpha^1 \sqrt{\frac{\xi-\alpha}{\xi}} f_1(\xi)\mathrm{d}\xi, \quad \frac{\delta_R}{\delta_0} = -\frac{\pi^2\alpha}{4} + \int_\alpha^1 \sqrt{\frac{\xi}{\xi-\alpha}} f_1(\xi)\mathrm{d}\xi \tag{7-8}$$

where

$$f_1(\xi) = -\frac{\mathrm{d}g}{\mathrm{d}\xi} = \frac{1}{2}\log\left|\frac{1+\sqrt{1-\xi}}{1-\sqrt{1-\xi}}\right| \tag{9}$$

and α is the extension of the reversed plastic zone (r_c), normalized with r_p (the monotonic plastic zone size at K_{max} for a stationary fatigue crack). Eqs. 7 and 8 in combination gives

$$\frac{\pi^2}{2} = \int_\alpha^1 \frac{f_1(\xi)}{\sqrt{\xi(\xi-\alpha)}}\mathrm{d}\xi. \tag{10}$$

Solving Eq. 10 numerically gives $\alpha = 0.9286$ and the residual stretch $\delta_R/\delta_0 = 0.8562$. Thus, in contrary to a stationary crack with a reversed plastic zone size of $r_p/4$, the reversed plastic zone size for a growing crack is less than $r_p/10$. Furthermore, the residual stretch left behind the growing crack is as high as 86% of the crack tip opening displacement for a stationary crack at K_{max}. It is now possible to study the unloading process from K_{max} with the assumption that there is no residual stretch, the crack opening displacement along the $x < 0$ will then vary with K as:

$$\frac{\delta}{\delta_0} = g\left(\frac{x}{r_p}\right) - \frac{2a_K}{r_p} g\left(\frac{x}{a_K}\right) \quad \text{where} \quad a_K = \frac{r_p}{4}\left(1 - \frac{K}{K_{max}}\right)^2 \tag{11)-(12)}$$

is the instantaneous size of the reversed plastic zone during unloading. Furthermore, Eq. 11 has a local minimum in the interval $(-\infty, 0)$. Attaching the residual stretch $\delta_R/2$ to each crack face, the first contact will occur when the left hand side of Eq. 11 is equal to δ_R/δ_0, at the location given by $\frac{d}{dx}\left(\frac{\delta}{\delta_0}\right) = 0$. The closure values $\xi_c = x_c/r_p$ and $\alpha_c = a_K/r_p$ are then given by:

$$g(\xi_c) - 2\alpha_c g\left(\frac{\xi_c}{\alpha_c}\right) = \frac{\delta_R}{\delta_0} \quad \text{and} \quad -f_1(\xi_c) + 2f_1\left(\frac{\xi_c}{\alpha_c}\right) = 0\,. \tag{13)-(14}$$

Solving Eqs. 13 and 14 analytically results in:

$$\alpha_c = \frac{1 - (\delta_R/\delta_0)^2}{4} \quad \text{and} \quad \xi_c = -\frac{4\alpha_c^2}{1 - 4\alpha_c}\,. \tag{15)-(16}$$

Eqs. 15 and 16 and Eq. 12 with $K = K_{cl}$ gives:

$$\frac{K_{cl}}{K_{max}} = 1 - \sqrt{1 - \left(\frac{\delta_R}{\delta_0}\right)^2}\,. \tag{17}$$

The above computed residual stretch $\delta_R/\delta_0 = 0.8562$ in Eqs. 15 - 17 gives: $\alpha_c = 0.0667$, $\xi_c = -0.0243$ and $\frac{K_{cl}}{K_{max}} = 0.483$. The closure model by Budiansky and Hutchinson provides a theoretical justification for the use of ΔK_{eff} to characterize fatigue crack growth. The model addresses just one of the crack closure effects (PICC). Another limitation is that the model is most appropriate for plane stress problems, whereas plane strain conditions are generally more relevant to fatigue crack growth,

especially in the near-threshold regime where the strongest effect of closure is usually observed.

Newman [11] proposed a modified model in which the plastic zone is built up of a large number of bars in the crack wake, thus being able to account for residual plastic deformation in the crack wake. Since this model is based on the Dugdale model it is not appropriate for plane strain, but this is accounted for by introducing an empirical fitting parameter. Unfortunately this violates the physical coupling.

4.4 Fatigue threshold and overload effects

With an increasing *R*-ratio the curve showing the typical fatigue crack growth behavior in ductile metals, shown in Fig. 5b, is moving left and slightly upwards. This means that the threshold value ΔK_{Ith} is decreasing with an increasing *R*-ratio. Thus, the threshold value is not a material parameter in the ordinary sense. This is explained by crack closure which is one of the factors that contributes to the threshold values. When the concept of crack closure is employed in the form of ΔK_{Ieff}, a threshold value is introduced in a natural way, *i.e* when $\Delta K_{\mathrm{Ieff}} \leq 0$. If there is an intrinsic, material specific, threshold value or not is not yet fully decided. Several researchers have developed models for estimating the intrinsic threshold based on dislocation emission from the crack tip or blockage of slip bands by grain boundaries [12, 13, 14]. This implies that the threshold measured in experiments is a result of crack closure and a possible intrinsic threshold. The contribution from crack closure is largely influenced by the microstructure and the environmental conditions when roughness-induced crack closure and oxide-indued closure mechanisms are largely involved near threshold, especially at low *R*-ratios.

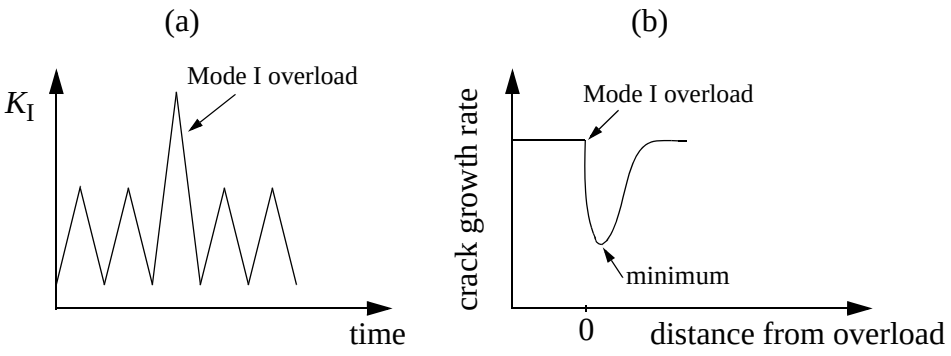

Figure 11 (a) Single Mode I overload during cyclic loading (b) schematic of retardation in crack growth rate following a single Mode I overload.

Consider the fatigue loading history shown in Fig. 11a. Constant amplitude loading is interrupted by a single Mode I overload cycle, after which the load is resumed with the same load level as before the overload (baseline load level). Prior to the overload steady state condition is reached, *i.e*. the closure level is constant. The overload cycle produces significantly larger plastic stretches. When the baseline load is resumed, the crack growth rate starts to drop reaching a minimum rate after some amount of growth. When the post-overload crack grows it leaves the large plastic stretches created by the overload in the plastic wake behind the crack tip. This leads to an increased PICC level, resulting in a crack growth rate reduction. Since the post-overload crack has to undergo some amount of growth before the overload stretches ends up in the plastic wake a delayed reduction is expected. This is also what is observed in experiments. Although there is a variety of experimental evidence supporting the role of PICC influencing retardation effects, many observations interprets that other mechanisms may also affect [5]: (i) crack tip blunting (ii) residual compressive stresses (iii) near threshold mechanisms. The first two mechanisms (i) and (ii) can not account for the delay in the retardation observed in the experiments, Fig. 11b. Experiments show that the retardation can persist when the post-overload crack has propagated through the overload zone of compressive residual stresses. Hence, mechanism (i) and (ii) alone can not be used to describe the retardation following an overload. When a fatigue crack is subjected to a tensile overload, the development of enhanced levels of PICC and possible residual compressive stresses results in a post-overload effective stress intensity factor range which is much lower than the baseline level. Therefore ΔK_{eff} may fall into the near-threshold regime even though ΔK_{base} is well into the Paris regime of fatigue crack

growth. This may activate additional mechanisms which are significant in near-threshold fatigue, *i.e*. stage I type of crack growth, roughness-induced crack closure and oxide-induced crack closure.

5. MIXED MODE I AND MODE II FATIGUE CRACK GROWTH

A crack in an isotropic linear elastic material subjected to an in-plane biaxial load, *i.e.* Mode I and II, results in a crack tip stress field given by the following equations:

$$\sigma_r = \frac{1}{\sqrt{2\pi r}}\cos\frac{\theta}{2}\left[K_I\left(1+\sin^2\frac{\theta}{2}\right)+\frac{3}{2}K_{II}\sin\theta-2K_{II}\tan\frac{\theta}{2}\right]$$

$$\sigma_\theta = \frac{1}{\sqrt{2\pi r}}\cos\frac{\theta}{2}\left[K_I\cos^2\frac{\theta}{2}-\frac{3}{2}K_{II}\sin\theta\right] \qquad (19)\text{-}(21)$$

$$\tau_{r\theta} = \frac{1}{2\sqrt{2\pi r}}\cos\frac{\theta}{2}\left[K_I\sin\theta+K_{II}(3\cos\theta-1)\right]$$

Here, K_I and K_{II} are tensile mode and shear mode crack tip stress intensity factors, respectively, (see Fig. 2) and (r, θ) are polar coordinates with origin at the crack tip, see Fig. 12.

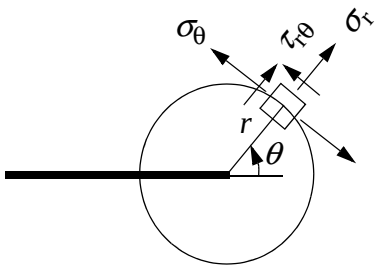

Figure 12 Polar stress components acting on a material element near the crack tip.

For life time prediction under mixed mode loading conditions the crack growth direction is of importance in order to estimate the crack growth rate. Several criteria have been proposed regarding the crack growth direction under mixed mode loading conditions [15]. One of the most used theories for mixed mode loading is the maximum tangential stress criterion (MTS criterion), proposed by Erdogan and Sih [16]. This criterion states that: (i) crack propagation starts from the crack tip along the radial direction, $\theta = \theta_0$, on which the tangential stress, σ_θ, becomes maximum (see Fig. 12); and (ii) fracture starts when the maximum tangential stress, σ_θ, reaches a critical stress, σ_c, equal to the fracture stress in uniaxial tension. Note that the stresses above must be related to a certain distance from the crack tip, because of the singularity. Mathematically, the condition for the crack growth direction can be expressed as:

$$\left.\frac{\partial \sigma_\theta}{\partial \theta}\right|_{\theta_0} = 0 \qquad \text{and} \qquad \left.\frac{\partial^2 \sigma_\theta}{\partial \theta^2}\right|_{\theta_0} < 0 . \tag{22)-(23)}$$

5.1 Proportional mixed Mode I+II loading

If Equations (19)-(21) are used to describe the stress field near the crack tip for a proportional mixed Mode I+II loading case, it can be shown that the MTS criterion (Eqs. 22 and 23) for the crack growth direction is the solution of the following equation: $\tau_{r\theta} = 0$, *i.e.*

$$K_I \sin\theta_0 + K_{II}(3\cos\theta_0 - 1) = 0 . \tag{24}$$

The deviation angle of the supplementary crack is then given by

$$\theta_0 = \pm \arccos\left(\frac{3K_{II}^2 + K_I\sqrt{K_I^2 + 8K_{II}^2}}{K_I^2 + 9K_{II}^2}\right), \tag{24}$$

where K_I and K_{II} are the stress intensity factors of the initial crack.

Gau *et al.* [17] studied the growth of fatigue cracks in four different metals. Particular attentions was paid to the mixed mode threshold behavior. In Fig. 13a a schematic of the fatigue fracture envelope for combined Mode I and Mode II crack growth in a stainless steel is shown. Here, ΔK_{II} is plotted against ΔK_I, both are nominal values normalized by the Mode I threshold, ΔK_{Ith}. The solid line in the figure indicates the lower bound threshold condition below which no crack growth was observed at a low *R*-ratio. The dashed curve indicates the mixed mode loading conditions at which formation of Mode I branch cracks occurred on a plane normal to the maximum hoop stress, σ_θ. Between these two curves so called co-planar growth occurred followed by crack arrest due to crack surface friction. Here, co-planar growth is mixed mode growth in the same direction as the starter crack, see Fig. 13b. Mode I crack branching appeared when the apparent nominal values of ΔK_I and ΔK_{II} corresponded to the upper bound curve. However, this curve appears to be strongly dependent on crack tip closure, crack surface contact, rubbing and oxide blocking. By increasing the load ratio, the upper bound curve approaches the lower bound. Two types of starter cracks were used. A 0.16 mm wide notch was formed in the specimens by spark erosion. In some tests a fatigue crack was grown from this notch under pure Mode I loading prior to the mixed mode loading, using a load reduction technique. When a notch, instead of a sharp fatigue crack, was subjected to mixed mode loading, the upper and lower bound curves coincided.

These results point to the significant role of frictional sliding in mixed mode fatigue crack growth. Gau *et al.* also found that, for certain combinations of mixed mode loading, the rate of crack growth was significantly effected by the so called *T*-stress. The *T*-stress is the first non singular stress term in the H.O.T-expression of Eq. 2. The *T*-stress is a constant stress acting parallel to the crack plane, in the direction corresponding to $\theta = 0$. Crack growth rates increased with increasing values of the *T*-stress at high ΔK_I-ΔK_{II}-load levels. The threshold fracture envelope though, was unaffected by the *T*-stress.

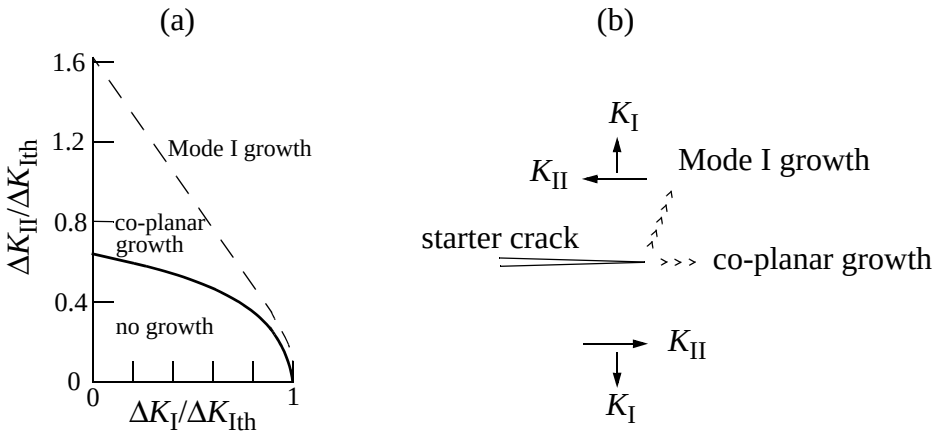

Figure 13 (a) Mixed mode threshold conditions for stainless steel, schematic after [17]. (b) The two growth types are indicated.

5.2 Non-proportional mixed Mode I+II loading

A widely discussed feature of non-proportional loading concerns the effect of superimposing a static Mode I load on cyclic Mode II loading [18], see Fig. 14a. Of particular interest is also the case where Mode I and Mode II load cycles are applied sequentially, instead of being superimposed, see Fig. 14b. These two combinations of loads have been reported to produce both co-planar crack growth and Mode I crack growth (growth perpendicular to the direction of the maximum tensile stress), depending on material and load ratio, K_I/K_{II} [18, 19, 20, 21]. Co-planar growth for the first loading case, mentioned above, is in the direction of the maximum shear stress range. In the second loading case, co-planar growth is both perpendicular to the maximum tensile stress of the Mode I part of the cycle and in the direction of the maximum shear stress for the subsequent shear part of the overall cycle. Doquet and Pommier [22] also studied the sequential load case with Mode I then Mode II on ferritic-pearlitic steel. Stable co-planar growth was observed from a mode-mixity $\Delta K_I/\Delta K_{II} = 1$ down to 0.25. At the higher mode-mixity, a synergetic effect was found, resulting in faster growth, compared to if contributions of each mode to the growth rate are simply added. Quite similar results were reported from [18 - 21], branch growth was observed when the tensile stress range dropped below about one-half of the shear range. Above, co-planar growth occurred instead and the rates were significantly higher. As mentioned in the Introduction, when the loading is non-proportional the orientation of the principal stress axes

rotates, *i.e*. the mixed mode ratio at the crack tip varies during the load cycle. Considering the MTS-criterion for non-proportional loading, it can be assumed that the crack propagates either in the direction corresponding to the $\sigma_{\theta,\max}$ or in the direction associated with the $\Delta\sigma_{\theta,\max}$, see Fig. 12.

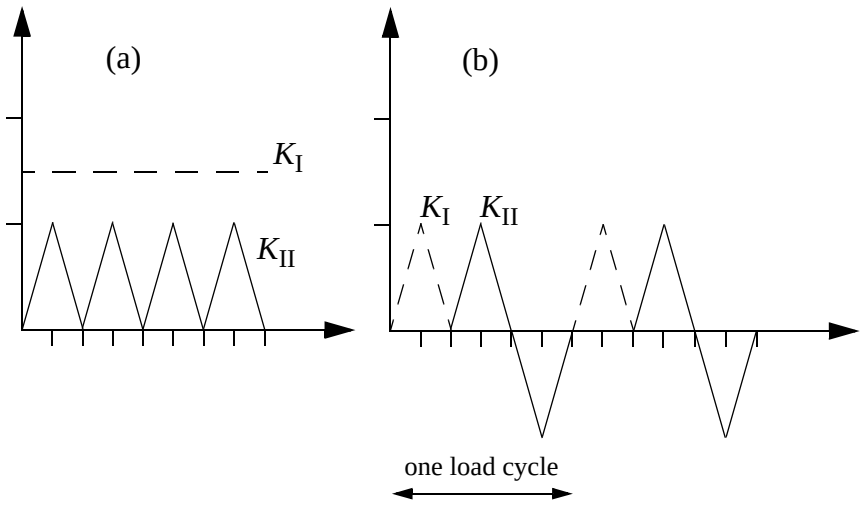

Figure 14 Examples of non-proportional loading.

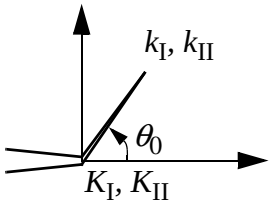

Figure 15 *K*-factors at deviated crack.

In 1980, Pook [23] studied non-proportional mixed mode. Without experimental proof, it was assumed that the crack would propagate in a direction in which the Mode I range would reach its maximum, Δk_{Imax}, see Fig. 15. In 1985 Hourlier *et al.* [24] performed an experimental study devoted to the prediction of crack path directions in multi axial fatigue. Two different types of materials, a steel alloy and an aluminum alloy, were investigated under non-proportional mixed Mode I/II loading. The experiments were performed on cruciform type specimens. It was shown that the two investigated materials exhibited very different crack bifurcation angles. Hourlier *et al.* concluded that: (i) in materials such as mild steel or structural steels exhibiting a small influence of *R*-ratio on Mode I crack growth rate, see Fig. 16a, the crack path is reasonably well predicted by a $\Delta\sigma_{\theta,\max}$ criterion. (ii) in materials such as high-strength aluminum alloys for which Mode I crack growth rates are largely influenced by the mean stress, see Fig. 16b, the crack path direction is governed not only by the range $\Delta\sigma_{\theta}$, but also by its maximum value $\sigma_{\theta,\max}$. The $\sigma_{\theta,\max}$-criterion which is an extension of a criterion for monotonic loading is expected to be applicable only at very high load levels. In this type of material and in the range of crack propagation rates investigated by Hourlier *et al.* which corresponds to the upper part of the Paris law regime, it is likely that the *R*-ratio effect is related to static fracture modes which are superimposed on fatigue fracture mechanism. To account for this behavior Hourlier *et al.* [24] proposed a new criterion $(\mathrm{d}a/\mathrm{d}N)_{\max}$. The criterion states essentially that fatigue cracks propagate in a direction in which the growth rate is maximum. The crack growth rate is computed from pure Mode I results. Assuming that the stress intensity factor k_{I} on the branched crack can be evaluated, see Fig. 15, the crack growth rate is found from $\mathrm{d}a/\mathrm{d}N(\theta) = f\,[k_{\mathrm{Imax}}(\theta), \Delta k_{\mathrm{I}}(\theta)]$ using conventional $\mathrm{d}a/\mathrm{d}N$ versus ΔK_{I} data at different *R*-ratios, like these presented in Fig. 16. In 1999, Plank and Kuhn [25] stated that under non-proportional mixed Mode I+II loading, two kinds of stable crack propagation may be distinguished. Experiments were performed on five different aluminum alloys and the results showed that an existing precrack will either kink, propagate in a Mode I controlled way, or exhibit co-planar propagation, *i.e.* Mode II controlled, see Fig. 17.

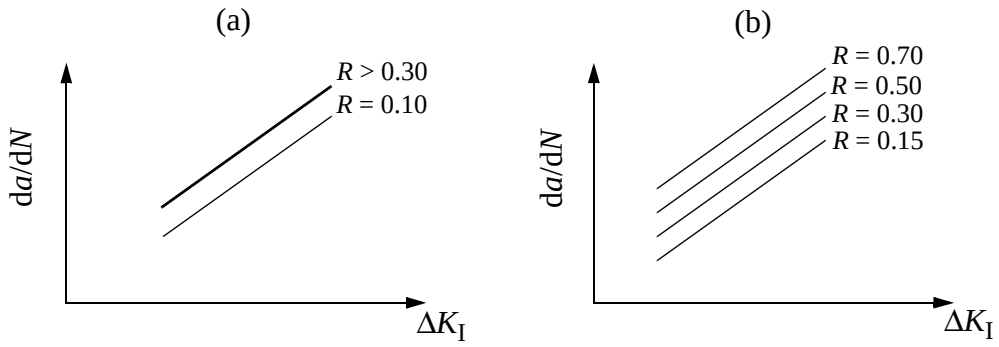

Figure 16 Schematic of the *R*-ratio effect for (a) structural steel alloy and (b) high-strength aluminum alloy, taken from experimental results presented by Hourlier *et al.* [24].

In Fig. 18 Plank and Kuhns [25] experimental results from one of the aluminum alloys, AA 2017, are presented, only showing the results from the specimens that kinked, *i.e.* where the crack growth was of local Mode I type. Three different types of non-proportional loading were performed: (A) Static Mode I + cyclic Mode II (B) Static Mode I + cyclic proportional mixed Mode I+II (C) Static Mode II + cyclic Mode I. The results are compared with the ordinary MTS_e-criterion (subscript e underlines that the criterion is based on the elastic stress field), shown in Fig. 18. The MTS_e-criterion predicts that all three load types should end up at the same curve, only load case B agrees. The results from the other aluminum alloys exhibit very similar results, except one which exhibit a fairly deviant behavior (this was the most ductile one).

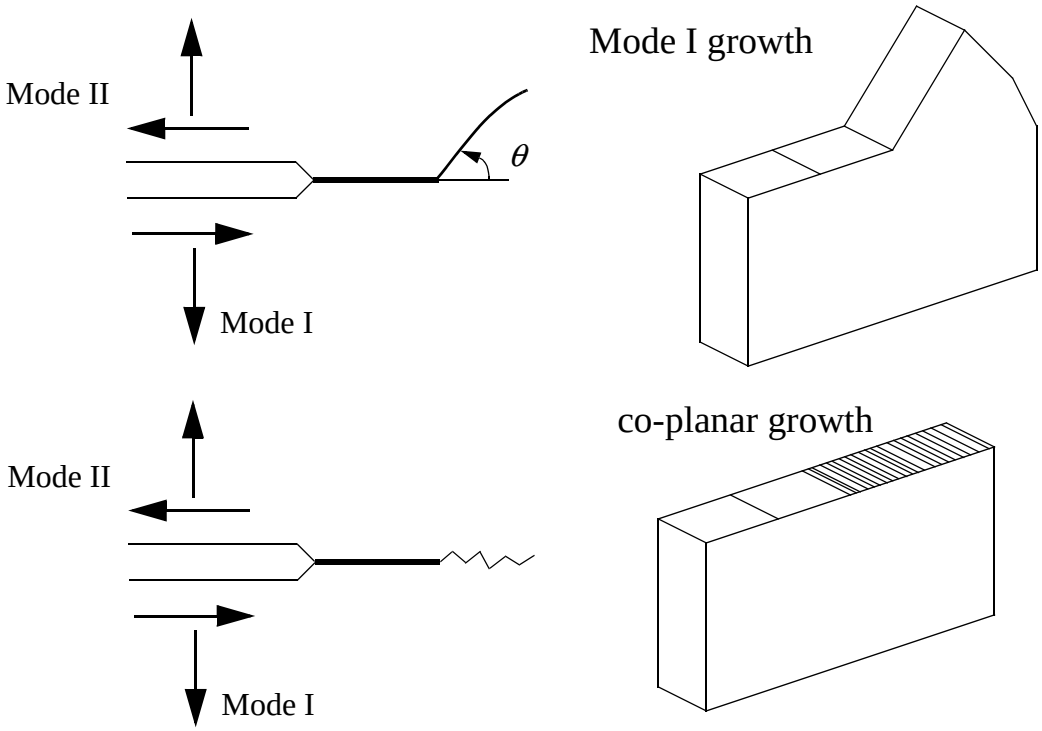

Figure 17 Different modes of crack growth.

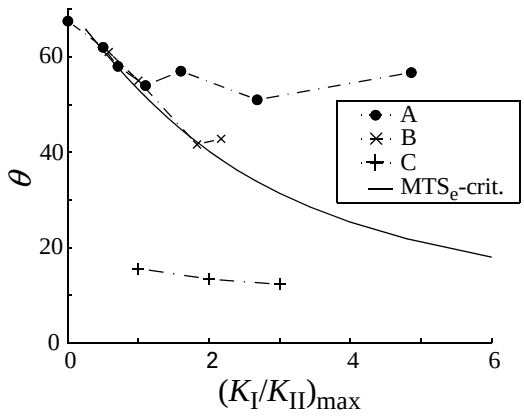

Figure 18 The crack deviation angles predicted by the MTS_e-criterion compared with Plank and Kuhns [25] experimentally observed results from the aluminium alloy 2017.

5.3 The new elasto-plastic MTS-criterion for crack path predictions presented in paper A

The effect of plasticity on the crack path direction under mixed mode non-proportional loading is investigated in paper A of this thesis. The analysis is based on finite element simulations where the elasto-plastic stress distribution at the crack tip is investigated. The plastic response is kinematic linear hardening with a very low hardening modulus, in order to simulate cyclic behavior. If the direction perpendicular to the maximum tangential stress is computed outside or inside the cyclic plastic zone under non-proportional loading the results will deviate, see Fig. 19. A new criterion is introduced, named MTS_p (subscript p for elastic-plastic). The criterion states that the crack will grow in the direction perpendicular to the maximum tangential stress on a radius, well inside the cyclic plastic zone, r_p. In order to find predictions that are independent of the radius chosen for evaluation, the radius, r_{eval}, has to be sufficiently small, otherwise the elastic field outside the plastic zone will influence the result. An example is shown in Fig. 20, where a static Mode I load is superimposed to cyclic Mode II loading (load case A, shown in Fig. 14a), $(K_I/K_{II})_{max} = 2$. The results show that for this load case $r_{p,min}/r_{eval} > 8$ results in radius-independent crack path predictions, see Fig. 20. Thus, according to Fig. 20, the predicted crack path direction for this load case is about 58°. The $r_{p,min}/r_{eval}$-ratio that results in radius independent predictions varies between the different load cases that have been analyzed. In the predictions presented in paper A, the $r_{p,min}/r_{eval}$-ratio was typically 20 - 30 in order to secure radius-independency.

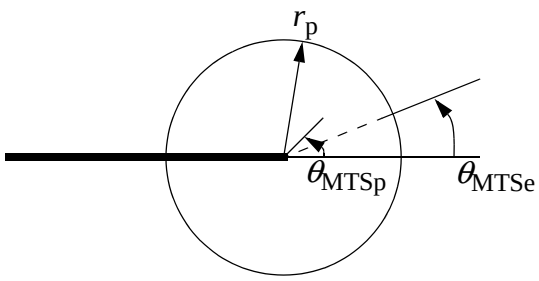

Figure 19 The direction perpendicular to the maximum tangential stress outside (e) and inside (p) the plastic zone.

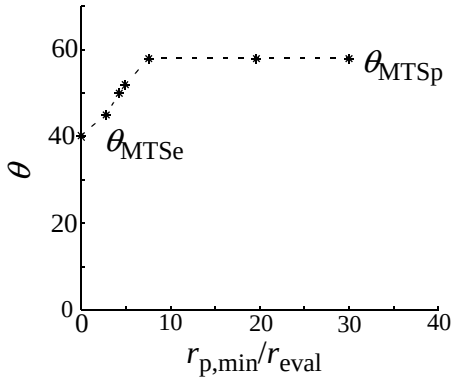

Figure 20 Finite element computations of the direction for the maximum tangential stress evaluated at different radii when a static Mode I load is superimposed to cyclic Mode II loading, $(K_I/K_{II})_{max} = 2$.

If the crack path is influenced by the maximum value of the tangential stress for some materials, like high-strength aluminum alloys, which was concluded by Hourlier *et al.* [24], the responsible mechanism acts most likely on the micro scale in the near crack tip region. Hence, when dealing with materials such as high-strength aluminum alloys at load levels where the maximum value of the tangential stress influence the crack path direction, the maximum value in the near crack tip region (MTS_p) seems more important than the maximum value outside the plastic zone (MTS_e). In Fig. 21a the computed crack path predictions using the MTS_p-criterion are compared with the experimentally observed results by Plank and Kuhn. Note, that the predictions from the ordinary MTS_e-criterion are shown in Fig. 18. In Fig. 21b the computed crack path predictions using the Maximum Tangential Stress Range criterion, MTSR, is compared with Plank and Kuhns results. Regarding the MTSR-criterion, the predictions are almost independent of whether the elastic ($MTSR_e$) or the elastic-plastic ($MTSR_p$) stress field is examined. The predictions from the MTS_p-criterion exhibit by far the best agreement with the experiments. Further results concerning crack paths are discussed in paper A.

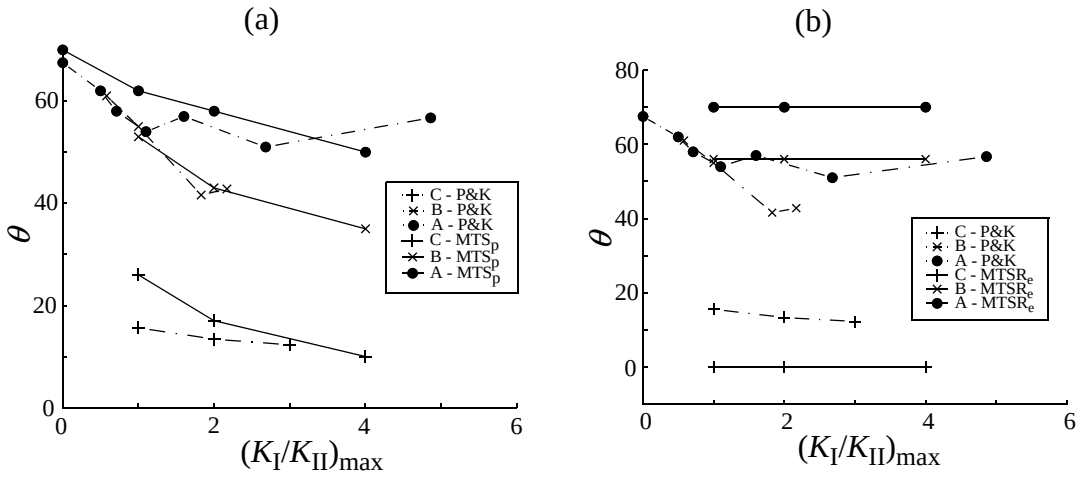

Figure 21 The crack deviation angles predicted by two stress based criteria compared with Plank and Kuhns [25] experimentally observed results from the aluminium alloy 2017. (a) MTS_p, (b) $MTSR_e$ (Maximum Tangential Stress Range, elastic stress field).

5.4 Effects of occasional Mode II loading on subsequent Mode I fatigue crack growth - presented in papers B and C

In 1987, Nayeb-Hashemi and Taslim [26] investigated the effects of Mode I and II overloads on subsequent Mode I crack growth. The result showed that in contrast to Mode I overloads, where the crack is either arrested or retarded, Mode II overloads give rise to crack growth rate acceleration, for a very short distance, with no retardation afterwards. In 1996, Gau and Upul [27] studied the effects of non-proportional overloading. The result from the experiment with Mode II overloading (ten overload cycles were applied in each test) exhibited a pronounced, long lasting retardation. This contradiction was the motivation for further investigations of this special load case. In papers B and C the effects of a single Mode II load on subsequent Mode I crack growth is investigated. Paper B is almost a purely experimental study. Paper C is an investigation concerning the reduction mechanisms, including both experiments and numerical modelling. The results of applying a single Mode II load cycle, with three different magnitudes, on steady state Mode I crack growth are shown in Fig. 22. The results clearly show that a single Mode II load cycle decreases subsequent Mode I crack growth rate.

The tendency though, indicates that there is a certain value (threshold) for the Mode II load, below which no reduction occurs. The main mechanism responsible for the reduction has, in papers B and C, been shown to be crack closure due to the Mode II displacement of the crack-surface roughness which causes mismatch between the upper and lower crack faces. In paper C a model based on both analytical and experimental results is developed for estimation of the degree of roughness-induced crack closure following a Mode II load. The analytical part of the model is based on the results presented in Section 4.3, *i.e.* the Dugdale model for describing the opening displacement of the crack surfaces. The fracture surface profile has been measured on one of the used specimens which was broken for Talysurf profiler measurements. The relative tangential displacement of the crack surfaces, $\delta_t(x)$, has also been measured experimentally at different crack lengths after the Mode II load. The measured fracture surface profile, displaced tangentially with the measured residual tangential displacement is treated like a residual stretch. The upper and lower crack faces are tangentially displaced $\delta_t(x)/2$ each, in opposite direction. This means that this additional "residual stretch" consists of two terms, one for the upper crack face and one for the lower, which are added to the analytical crack opening displacement, see Fig. 23. It is now possible to study the unloading process and estimate the crack closure level numerically, *i.e.* the first contact between the tangentially displaced surface roughness on the upper and lower crack faces. This estimated closure level includes both the effects of roughness-induced crack closure and plasticity-induced crack closure, RICC and PICC, respectively.

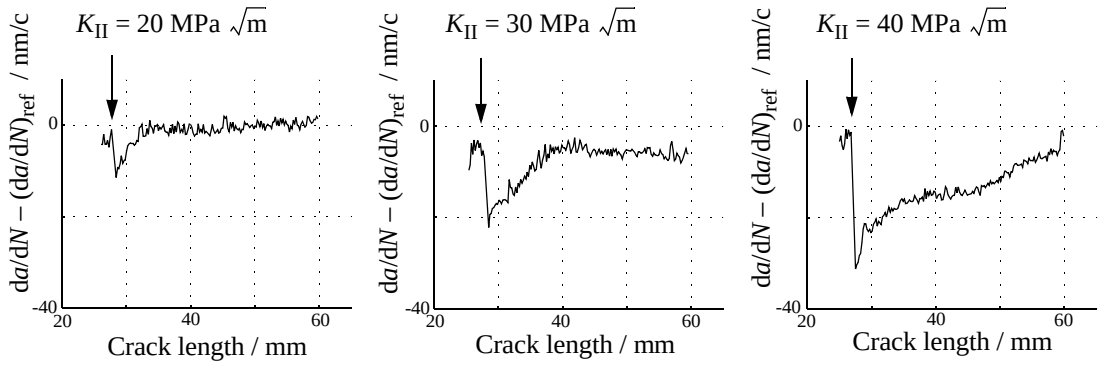

Figure 22 Change in Mode I crack growth rate due to a single Mode II load cycle of three different magnitudes (ΔK_I = 20 MPa$\sqrt{m}$, R = 0.1).

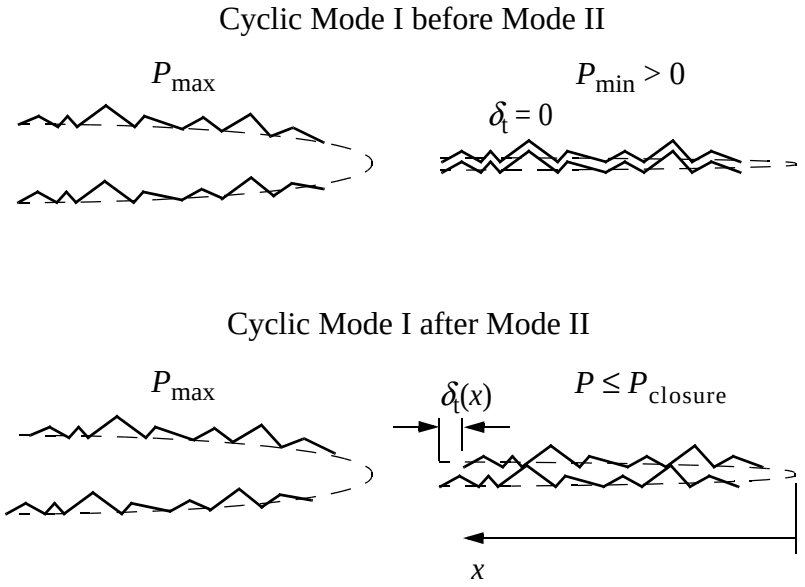

Figure 23 Schematic of the RICC estimation, due to a Mode II load, using the model in paper C. The dashed lines are the crack opening profiles, estimated using an analytical expression in the model. The bold lines are the fracture surfaces. In the model, the experimentally measured fracture surface profile is used. The relative tangential displacement of the crack surfaces, δ_t, is measured experimentally as a function of x.

5.5 Effect of periodic Mode II loading on Mode I fatigue crack growth - paper D

In papers B and C the effect of a single Mode II load cycle on subsequent Mode I crack growth was studied. As mentioned in Section 5.2, Bold, Wong, Brown and Allen [18, 19, 20, 21] and Doquet and Pommier [22] have investigated a special case of sequential mixed Mode I and II loading, with load blocks containing a Mode I load followed by a Mode II load cycle with $R_{II} = -1$ ($R_{II} = K_{IImin}/K_{IImax}$), see Fig. 14b. The load cases in between these two, *i.e*. Mode I crack growth with periodic Mode II loading, has not been investigated in the literature at all. In paper D, a series of experiments have been performed in order to investigate Mode I crack growth with periodic Mode II loading, *i.e*. different cases of sequential mixed Mode I and II loading. The loading was applied to the specimens using a new type of loading device. The influence on the crack growth rate for three parameters have been investigated, the Mode I *R*-ratio, the magni-

tude of the Mode II loads and the Mode II periodicity, M = number of Mode I load cycles per Mode II load. The influence from each of these parameters have been examined separately. The Mode II load has to be large enough to create residual displacements otherwise no effect at all occurs, irrespective of the other two parameters mentioned above. Two mechanisms are found, roughness-induced crack closure (RICC) that reduces the crack propagation rate and a Mode II related damage mechanism that increases the crack growth rate temporary at every Mode II load. This implies that for large Mode II periodicity, M, the crack growth rate is reduced and for low Mode II periodicity, M, the growth rate is increased. It is also possible to find a minimum crack growth rate for a certain Mode II periodicity, M*, when the parameters K_{II} and R are kept constant, see Fig. 24a. The influence of the Mode II-magnitude is shown in Fig. 24b. At high R-ratios the reduction mechanism disappears and consequently the crack growth rate increases when periodic Mode II loading is applied, see Fig. 24c.

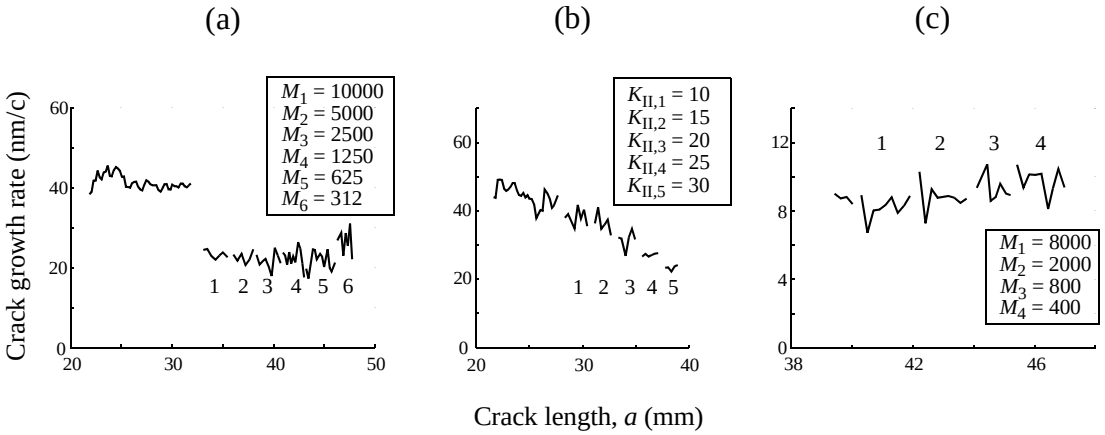

Figure 24 Results from experiments presented in paper D. The rate of Mode I crack growth with periodic Mode II loading with, (a) $\Delta K_I = 20\ \text{MPa}\sqrt{\text{m}}$, $R = 0.1$, $K_{II} = 30\ \text{MPa}\sqrt{\text{m}}$ and the Mode II periodicity, M, is ranging from 10000 to 312, (b) $\Delta K_I = 20\ \text{MPa}\sqrt{\text{m}}$, $R = 0.1$, $M = 2500$ and the Mode II magnitude is ranging from 10 to 30 $\text{MPa}\sqrt{\text{m}}$, (c) $\Delta K_I = 12\ \text{MPa}\sqrt{\text{m}}$, $R = 0.58$, $K_{II} = 30\ \text{MPa}\sqrt{\text{m}}$ and M ranging from 8000 to 400. The result of the pure Mode I crack growth prior to the periodic Mode II loading is shown in each figure.

6. DISCUSSION AND OUTLOOK

As mentioned in the Introduction, the subject of fatigue is huge, so is the sub-topic non-proportional mixed mode loading that has been in focus in this thesis. The work presented here deals with a fraction of the possible load cases in the area of non-proportional mixed mode loading. These load cases are important partly because they occur in load carrying structures and partly because some of them are convenient for examination of important fatigue mechanisms. In paper A, it was found, using FE-simulations, that plasticity effects have to be considered in order to predict the crack path in non-proportional mixed mode fatigue. Comparisons were made with experimental results taken from the literature. The experimental part of this thesis is limited to sequential mixed mode (SMM) loading, in Mode I and Mode II. It is shown in papers B, C and D that most phenomena associated with SMM-loading can be explained by the introduction of RICC.

The MTS_p-criterion can be used in extended FE-modeling, including for example remeshing for simulating crack growth, for crack path predictions of long growth. In, addition, other constitutive relations may be employed.

Since the subject of non-proportional loading is relatively unexplored, further research is needed in order be able to perform safe fatigue life predictions. More related to this work, further research is needed to investigate the mechanisms in SMM-fatigue, especially at low *M*-values, where the acceleration mechanism is significant. Further research is also needed to understand the mechanisms that influence the crack path directions in non-proportional fatigue.

The dual mode loading device, presented in paper D, is very convenient to use when studying SMM-fatigue. The loading device can be used to study any combination of sequential mixed Mode I/II loading, *e.g.* varying load blocks with variable amplitude, both for Mode I and Mode II.

The model presented in paper D can be extended to include additional parameters for more reliable predictions of the average crack growth rate in SMM-loading.

7. REFERENCES

[1] www.airdisaster.com/photos/aloha243/7.shtml

[2] P. C. Paris, M. P. Gomez and W. E. Anderson (1961). A rational analytic theory of fatigue. The Trend in Engineering 13, 9-14.

[3] Hibbitt, Karlsson and Sorensen, INC, ABAQUS 6.2.

[4] W. Elber (1970). Fatigue crack closure under cyclic tension. Engng Fracture Mech. Vol. 2, 37-45.

[5] S. Suresh. Fatigue of Materials, Second edition (1998), Cambridge University Press, Cambridge, U.K.

[6] K. Donald and P. C. Paris (1999). An evaluations of ΔK_{eff} estimation procedures on 6061-T6 and 2024-T3 aluminium alloys. Int. J. Fatigue, 47-57.

[7] R. C. McClung and H. Sehitoglu (1989). On the finite element analysis of fatigue crack closure-1. Basic modeling issues. Engng Fract. Mech. No.2, 33, 237-252.

[8] R. C. McClung, B. H. Thacker and S. Roy (1991). Finite element visualization of fatigue crack closure in plane stress and plane strain. Int. J. Fract. 50, 27-49.

[9] S. Roychowdhury and R. H. Dodds Jr. (2003). Three-dimensional effects on fatigue crack closure in the small-scale yielding regime. Fatigue Fract. Engng Mater. Structs, 26, 663-673.

[10] B. Budiansky and J. W. Hutchinson (1978). Analysis of closure in fatigue crack growth. J. Appl. Mech., 45, 267-276.

[11] J. C. Newman, Jr. (1981). A crack-closure model for predicting fatigue crack growth under aircraft spectrum loading, ASTM STP 748, ASTM, West Conshohocken, Pa., 53-84.

[12] T. L. Anderson (1991). Fracture mechanics fundamentals and applications, CRS Press, Boca Raton, U.S.A.

[13] T. Yokobori, A. T. Yokobori Jr. and A. Kamei (1975). Dislocation dynamic theory for fatigue crack growth. Int. J. Fract., Vol. 11, 781-788.

[14] K. Tanaka, Y. Akiniwa and M. Yamashita (1981). Fatigue growth threshold of small cracks. Int. J. Fract., Vol. 17, 519-533.

[15] D. F. Socie and G. B. Marquis (2000). *Multiaxial Fatigue*, SAE International. Printed in U.S.A.

[16] F. Erdogan and G. C. Sih (1963). On the crack extension in plates under plane loading and transverse shear. J. Basic Engng, 85, 519-25.

[17] H. Gau, N. Alagok, M. W. Brown and K. J. Miller (1985). Growth of fatigue cracks under combined Mode I and Mode II loads. Multiaxial Fatigue, ASTM 853 (Edited by K. J. Miller and M. W. Brown), pp. 184-202. American Society for Testing and Materials, Philadelphia, Pa.

[18] P. E. Bold, M. W. Brown and R. J. Allen (1992). A review of fatigue crack growth in steels under mixed mode I and II loading. Fatigue Fract. Engng Mater. Structs, 15, 965-77.

[19] P. E. Bold, M. W. Brown and R. J. Allen (1991). Shear mode crack growth and rolling contact fatigue. Wear, 144, 307-317.

[20] S. L. Wong, P. E. Bold, M. W. Brown and R. J. Allen (2000) Fatigue crack growth rates under sequential mixed-mode I and II loading cycles. Fatigue Fract. Engng Mater. Structs, 23, 667-674.

[21] S. L. Wong, P. E. Bold, M. W. Brown and R. J. Allen (1996) A branch criterion for shallow angled rolling contact fatigue cracks in rails. Wear, 191, 45-45.

[22] V. Doquet and S. Pommier (2004) Fatigue crack growth under non-proportional mixed mode loading in ferritic-pearlitic steel. Fatigue Fract. Engng Mater. Structs, 27, 1051-1060.

[23] L. P. Pook (1980). The significance of mode I branch cracks for combined mode failure. Glasgow: National Engineering Laboratory.

[24] F. Hourlier, H. d'Hondt, M. Truchon, A. Pineau (1985). Fatigue crack path behavior under polymodal fatigue. Multiaxial Fatigue, ASTM 853 (Edited by K. J. Miller and M. W. Brown), pp. 228-247. American Society for Testing and Materials, Philadelphia, Pa.

[25] R. Plank, G. Kuhn (1999). Fatigue crack propagation under non-proportional mixed mode loading. Engng Fract. Mech., 62, 203-229.

[26] H. Nayeb-Hashemi and M. E. Taslim (1987). Effects of the transient mode II on the steady state crack growth in mode I. Engng Fract. Mech., Vol. 26, No. 19, 789-807.

[27] H. Gao, S. F. Upul (1996). Effect of non-proportional overloading on fatigue life. Fatigue Fract. Engng Mater. Structs, 19, 1197-1206.